BiCMOS microfluidic sensor for single cell label-free monitoring through microwave intermodulation

Palego, Cristiano

Microwave Symposium (IMS), 2016 IEEE MTT-S International

DOI:
10.1109/MWSYM.2016.7540266

Published: 11/08/2016

Peer reviewed version

BiCMOS Microfluidic Sensor for Single Cell Label-Free Monitoring Through Microwave Intermodulation

C. Palego[1], G. Perry[1], C. Hancock[2], F. Hjeij[3], C. Dalmay[3], A. Bessaudou[3], P. Blondy[3], A. Pothier[3], F. Lalloue[4], B. Bessette[4], G. Begaud[4], M-O. Jauberteau[4], C.B. Kaynak[5], M. Wietstruck[5], M. Kaynak[5], M. Casbon[6], J. Benedikt[6], D. Barrow[6], A. Porch[6]

[1]Bangor University, Bangor, UK, [2]Creo Medical Ltd., Chepstow, UK, [3]XLIM, Limoges, France, [4]EA 3842 Limoges University, Limoges, France, [5]IHP Microelectronics, Germany, [6]Cardiff University, Cardiff, UK

Abstract — A novel microfluidic biosensing platform based on Bipolar-Complementary Oxide Semiconductor (BiCMOS) technology is presented. The device relies on a quadruple electrode system and a microfluidic channel that are directly integrated into the back-end-of-line (BEOL) of the BiCMOS stack. For proof of concept repeatable electrical trapping of single SW620 (colon cancer) cells in the quadruple electrode system is initially demonstrated. Additionally, for the first time a microwave intermodulation technique is used for high sensitivity dielectric spectroscopy, which could pave the way to label-free monitoring of intracellular processes and manipulation such as electroporation.

Index Terms —Biosensor, BiCMOS, cell modeling, coplanar wave-guide, electroporation, microwave, non-linearity.

I. Introduction

Silicon based microfluidic systems attract increasing interest due to the potential for new and high performance Lab-On-Chip (LOC) functionalities. For example, state-of-the-art BiCMOS technology [1] allows combining microfluidic switches, pumps and mixers on the same chip while supporting low-parasitic and millimeter-wave range sensing. This is not only key to gaining insight regarding individual biological cells with unprecedented specificity [2]; it is also expected to enhance microwave spectroscopy [3] and manipulation techniques concurrent to the optimization of single cell delivery [4] and on-chip interferometry [5].

Among such techniques electroporation [6] is of interest for cell viability, function and drug delivery control. Yet, on-chip analysis of electroporation is primarily conducted through cytotoxic dye probing and fluorescence spectroscopy. Additionally, electrical monitoring of cell response through linear electrical analysis is (e.g. scattering parameters) can be impaired by the very low signal-to-noise ratios (SNR) [7].

A novel silicon silicon-based biosensing chip and non-linear electrical analysis were used in this work to demonstrate high-SNR monitoring of cell properties and processes such as electroporation.

II. Origin of Non-Linearity

As a first order approximation, the maximum transmembrane potential (TMP) induced by an alternating

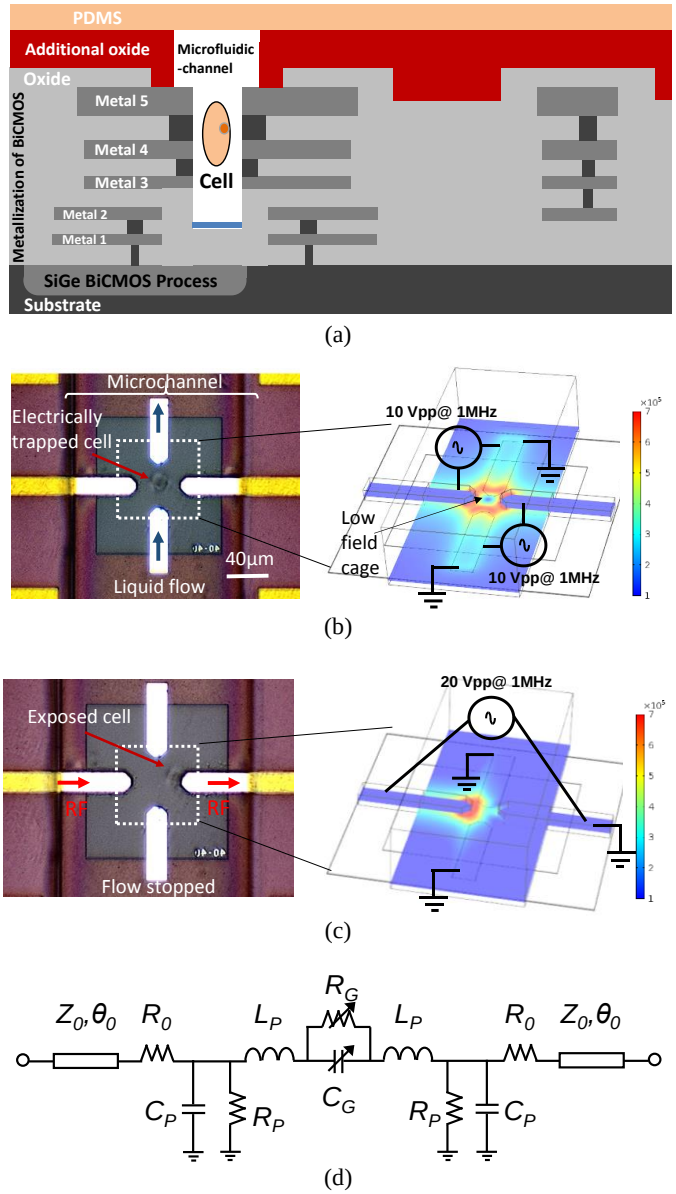

Fig. 1. (a) Cross-sectional view of the microfluidic platform integrated into a standard BiCMOS process. The 4-electrode system with a single cell and biasing arrangement during (b) trapping and (c) exposure/sensing along with its equivalent circuit model.

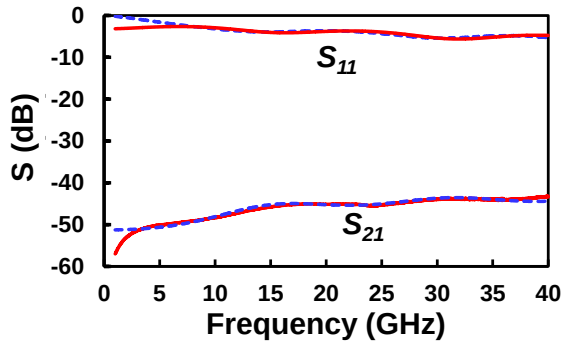

(a)

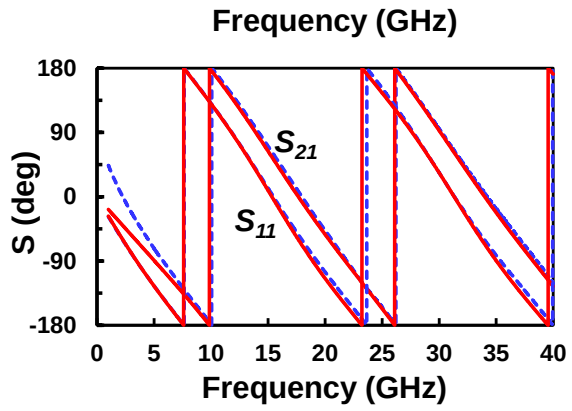

(b)

Fig. 2. Measured (solid) and modeled (dashed) (a) magnitude and (b) phase of the scattering parameters with the microchannel filled by the sucrose solution and prior to cell injection.

electric field E that is applied to a cell in the capacitive gap of the quadruple electrode structure in Fig.1 (a-c) can be modeled by [8]:

$$TMP = aRE/[1 + (2\pi f\tau)^2]^{1/2} \quad (1)$$

where a is a dimensionless factor which depends on the cell geometry, R is the cell radius and τ is a time constant. For SW620 cells R ~7.5 μm and the parameters in Table 1 result in a TMP~1V under a 1 MHz, 10V (20 Vpp) sinusoidal signal applied across a 40 μm gap (E=2.5 KV/cm).

Under such field conditions, electrostatic tractions are generated along the interfaces between the membrane and surrounding media leading to local membrane deformation and change of dielectric properties. Nanopores are thought to form in the plasma membrane for TMP ranging from 0.1 to 1V and enable the outpouring of the intracellular ionic content [6]. Such modification in turn, changes the local electric field and hence the electrostatic tractions through a feedback mechanism that resembles the voltage-force-capacitance relationship in a micro-electromechanical switch. Therefore such dynamics can be investigated through standard non-linear characterization [9] and the device shown in Fig. 1 to ensure precise cell delivery.

TABLE I
APPLIED LF/RF SIGNALS, DEVICE AND CELL PARAMETERS @ 0/360S AFTER STIMULUS APPLICATION

Parameter	Value
P_{RF} (mW) @15 GHz	10
V_{RF} (V_{pp}) @1 MHz	10
R_0 (Ω)	17.6
Z_0 (Ω)	44
θ_0 @ 15 GHz (°)	152.1
C_P (fF)	120
R_P (fΩ)	260
L_P (nH)	1.8
R_G (kΩ)	23/21.3
C_G (fF)	1.1/1.0
a	1.74
τ(μs)	0.5

III. CHIP DESIGN, CELL PREPARATION AND TRAPPING

A. Electrode and Microchannel Design

The BEOL of the 0.25 μm standard BiCMOS process was modified to fabricate the microchannel and the 3D microelectrodes for cell trapping, stimulation and sensing. The microfluidic channel with a depth and width of 15 μm, 150 μm, respectively, was formed via DRIE of oxide in the BEOL. The trapping microelectrode fabrication involved stacking the three last metal levels of the BEOL (Metal5, Metal4 and Metal3) and interconnecting them through a dense mesh of metallic vias across SiO2 layers, as shown in Fig. 1(a).

Four 3D electrodes with overall thickness of up to 9 μm were implemented in the middle of the microfluidic channel to ensure efficient trapping and RF probing of flowing cells. Metal2 and Metal1 were not used in order to minimize the coupling to the substrate which would impair the RF sensing. The two thickest (9 μm) electrodes were used to apply both the dielectrophoresis (DEP) and the RF signals to flowing particles. The two thinnest (0.45 μm) electrodes, implemented perpendicularly in the middle of the microfluidic channel, were electrically grounded to form an electrical potential cage with insignificant perturbation of the liquid flow. A 3-mm thick PDMS layer was used for sealing of the microfluidic channel while enabling optical transparency.

B. Cell Preparation

SW620 (colon cancer) cells were conventionally grown in cell culture flask (37 °C in a humidified 5% CO2 – 95% air incubator) for two days. They were then suspended in a DI water/sucrose isotonic solution with 20 mS/m conductivity. The suspension medium was injected in the microchannel through the flow control system for broadband calibration.

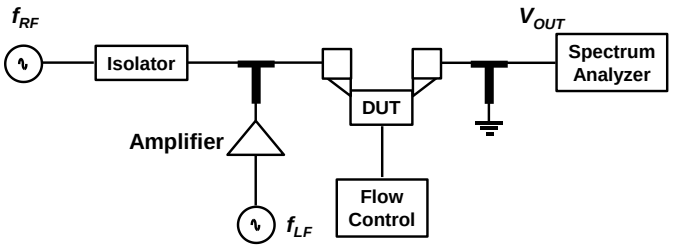

Fig. 3. Microwave intermodulation measurement setup.

After centrifugation and re-suspension cells were injected in the microchannels for trapping and RF characterization.

C. Single Cell Trapping

The quadruple electrode design formed an efficient electrical trap for single particles that reacted to negative DEP (i.e. for particles showing lower permittivity than the medium flowing in the microfluidic channel). Indeed, since the electric field distribution presents a minimum in the middle of the structure (Fig.1(b)), when the flowing cells passed between the thick microelectrodes they were slowed down and stopped under a DEP sinusoidal signal magnitude of 5V (10 Vpp) at 1 MHz. Eq. (1) and staining essays [7] suggest that cells poration due to the trapping signal is unlikely. After cell trapping the microfluidic flow was interrupted, cells were immobilized and the RF and LF frequency signals were injected through a bias-Tee at the input port as in Fig. 3.

IV. Experimental Results

A. Linear Analysis: Scattering Parameters

Fig 2 shows the measured magnitude and phase of the scattering parameters response from the chip with the suspension medium filling the microchannel. The measured performance was fitted using the broadband circuit model that is shown in Fig. 1(c). There, Z_0, θ_0, R_0, represent the feeding microstrip line characteristic impedance, electrical length and resistance, respectively. C_P, R_P, L_P model the fringe shunt capacitance and resistance along with the series inductance associated to the microstrip line discontinuity. C_G, R_G, represent the capacitance and resistance in the capacitive gap, which depend on the cell presence and properties. However, it should be noticed that (linear) scattering parameters analysis results in variations as small as 0.01 dB when single cells are trapped in similar capacitive gap structures [4, 9]. Vanishingly small differences are also relied upon to discriminate single cells type and viability. Hence, while the scattering response in Fig. 2 was recorded before cell injection, the response after a single cell was trapped is only marginally different, which makes accounting of the cell contribution to C_G, R_G parameters challenging.

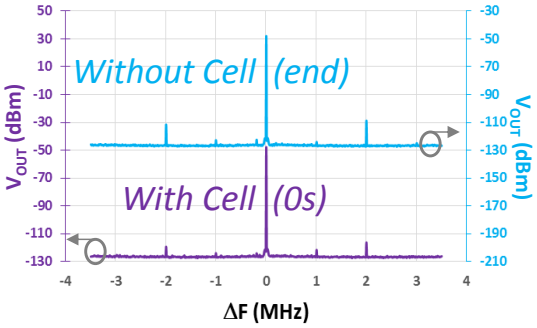

(a)

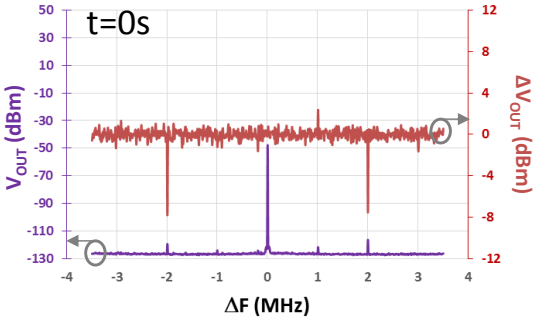

(b)

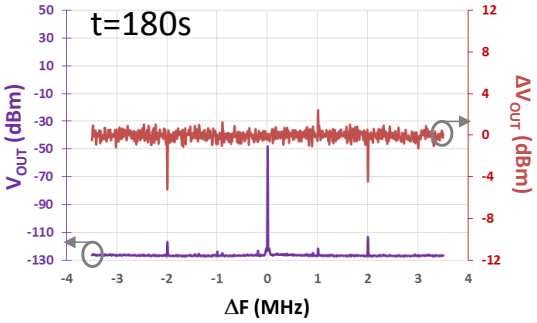

(c)

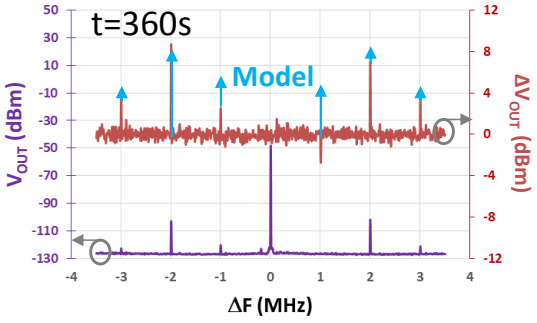

(d)

Fig. 4. Spectral response with and without a trapped cell (a) under the RF carrier only and under combined RF+LF stimulation (b) at 0s, (c) a180s, and (d) at 360s which also includes the model prediction.

B. Non-linear Analysis: Microwave Intermodulation

As expected, the harmonic response recorded with the only 15 GHz 10 mW RF carrier featured no sidebands and is not reported here. Conversely, Fig. 4 shows that clearly detectable sidebands were recorded upon superposition of the LF 1MHz 10V sinusoidal signal to the 15 GHz carrier via the bias-Tee. Such stimulus resulted in an LF electric field amplitude comparable to [6] and cells were additionally seen to move towards the E-field minimum as shown in Fig 1(c).

The absolute signals recorded with and without a cell in the capacitive gap are shown in Fig. 4(a). The response without any trapped cell was recorded at the end of the test (7 minutes) and used as baseline when plotting the deviation of the curves recorded at different times in Fig. 4(b-d). The cell presence resulted in significantly different sideband levels (>1 dB at $+1f_{LF}$, <-6dB at $\pm 2f_{LF}$), although a marginal decrease in the baseline was also recorded. This was attributed to the smaller series capacitance when a cell replaced the high permittivity medium across the capacitive gap of the sensor.

The harmonic response was periodically sampled every 15 seconds between 0s, when the LF signal was switched on, and 7 minutes, when the test was interrupted. The response recorded between 0s and 360 s showed consistently: 1) no $\pm 3f_{LF}$ components 2) smaller $\pm 2f_{LF}$ components 3) comparable $-1f_{LF}$ component but larger $+1f_{LF}$ component than in the reference signal. Fluctuations of the sideband levels with respect to the baseline signal are visible in Fig. 4(b-c) and were recorded at intermediate times, however the sign of the deviation signal never changed. A sizeable (~10dB) increase in the $\pm 2f_{LF}$ harmonics along with the clear appearance of $+3f_{LF}$ components (~4dB) was observed at 360s, as visible in Fig. 4(c). The appearance of a $-1f_{LF}$ component along with sign reversal of the $+1f_{LF}$ component can be also noticed. Such behavior was maintained over the following 2 minutes after which the test was finally stopped. Several SW620 cells provided repeatable harmonics but somehow different onset times.

The spectrum at 360s also shows that the measured intermodulation variation was qualitatively matched by the circuit model in Fig. 1 (b), where a step-like discontinuity is enforced both in the C_G and in the R_G parameters. Such variation is consistent with the capacitance difference between a live and a dead cell [6, 10] and with a sudden increase in the medium conductivity due to intracellular ions outpouring [6]. Both facts are compatible with a compromised membrane integrity ensuing electroporation, although further evidence could be only collected through fluorescence analysis. Nonetheless the present technique underscores the potential for high sensitivity, real-time and label-free monitoring of intracellular processes and manipulation. Indeed, faster sampling of the spectral response could potentially allow overcoming the fluorometry's tradeoff between fluorescence $\Delta f/f$ sensitivity and die response time.

CONCLUSION

A novel BiCMOS microfluidic chip was developed and applied to precise single cell trapping and functional monitoring through a microwave intermodulation technique. While such technique would need to be coupled to conventional fluorescence analysis for further validation, its potential for real-time, label free and high sensitivity spectroscopy can be appreciated from this preliminary study.

ACKNOWLEDGEMENT

The Authors gratefully acknowledge the financial support provided by the Welsh Government and Higher Education Funding Council for Wales through the Sêr Cymru National Research Network in Advanced Engineering and Materials, as well as by the Region Limousin Council & FEDER.

REFERENCES

[1] M. Kaynak, M. Wietstruck, C. Kaynak, S. Marschmeyer, K. Schultz, H. Slitz, A. Kruger, R. Barth, K. Schmalz, G. Gastrock, B. Tillack "BiCMOS Integrated Microfluidic Platform for Bio-MEMS applications," *IMS*, pp.1-3, 1-6 Jun. 2014.

[2] A. Martellosio, M. Pasian, M. Bozzi, L. Perregrini, A. Mazzanti, F Svelto, P. Sumers, G. Renne, M. Bellomi "0.5-50 GHz dielectric characterisation of breast cancer tissues," *Electronics Lett.*, *51*(13), pp.974-975, Jun. 2015.

[3] L.Y. Zhang, C. Bounaix Morand du Puch, C. Dalmay, A. Lacroix A. Landoulsi, J. Leroy, C. Mellin, F. Lalloue, S. Battu, C. Lautrette, S. Giraud, A. Bessaudou, P. Blondy, M-O. Jaubertau, A Pothier "Discrimination of colorectal cancer cell lines using microwave biosensors" Sensors & Actuators: A. Phys, 216(1), pp. 405-16, Sept. 2014.

[4] K. Grenier, D. Dubuc, T. Chen, F. Artis, T. Chretiennot, M. Pupot, J. Fournie, "Recent advances in microwave based dielectric spectroscopy at the cellular level for cancer investigation," in *IEEE Trans. Microw. Theory Techn.*, vol. 61(15), pp.2023-30, Apr. 2013.

[5] J-C. Chien, , M. Anwar, L. Lee E-C. Yeh, M. Niknejad "A 6.5-17.5 GHz dual-channel interferometer-based capacitive sensor in 65-nm CMOS for high-speed flow cytometry," *IEEE Int.Microwave Symp. Dig*, pp.1-3, Jun. 2014.

[6] S. C. Bürgel, C. Escobedo, N. Haandbaek, A. Hierlemann "On-chip electroporation and impedance spectroscopy of single cells." *Sensors and Actuators B: Chem.*, vol. 210, pp. 82-90, Apr. 2015.

[7] C. Palego, C. Merla, Y Ning, C. Multari, X. Cheng, D. Molinero, G. Ding, X. Luo, J. Hwang, "Broadband microchamber for electrical detection of live and dead biological cells", *IEEE* Int. Microwave Symp. Dig. pp.1-3, Jun. 2013.

[8] P. Marszalek, D. Liu, t. Tsong "Schwan equation and transmembrane potential induced by alternating electric field.," *Biophys. J.*, vol. 58, (4), pp. 1053–8, Oct. 1990.

[9] C. Palego, S. Hadler, B. Baloglu, Z. Peng, J. Hwang, H. Nied, D. Forehand, C. Goldsmith "Microwave intermodulation technique for monitoring the residual mechanical stress in RF MEMS capacitive switches", *IEEE Int. Microwave Symp. Dig.*, pp.29-32, Jun. 2008.

[10] X. Ma, X. Du, C. Multari, Y. Ning, C. Palego, X. Luo, V. Gholizadeh, X. Cheng, J. Hwang "Broadband single-cell detection with a coplanar series gap," *Microwave Meas. Conf. 2015 86th RFTEG.*, Dec. 2015.